Available online at www.sciencedirect.com
ScienceDirect
Biomaterials 29 (2008) 834–843
Biomaterials
www.elsevier.com/locate/biomaterials

Influence of electrospun collagen on wound contraction of engineered skin substitutes

Heather M. Powell[a,*], Dorothy M. Supp[a,b], Steven T. Boyce[a,b]

[a]*Research Department, Shriners Burns Hospital, Cincinnati, OH, USA*
[b]*Department of Surgery, College of Medicine, University of Cincinnati, Cincinnati, OH, USA*

Received 20 July 2007; accepted 25 October 2007
Available online 3 December 2007

Abstract

The treatment of massive full-thickness burns with engineered skin substitutes has shown promise in clinical trials. The majority of skin substitutes are comprised of fibroblasts and/or keratinocytes on collagen scaffolds, commonly generated by freeze drying which can generate significant structural heterogeneity. Electrospinning may generate collagen scaffolds with greater homogeneity. Skin substitutes were fabricated using either freeze-dried (FD) or electrospun (ES) collagen scaffolds. Cell distribution, proliferation, organization, and maturation were assessed on each scaffold type *in vitro*, and engraftment and healing of full thickness wounds in athymic mice were tested. *In vitro* evaluation of freeze-dried collagen skin substitutes (FCSS) and electrospun collagen skin substitutes (ECSS) revealed no significant differences in cell proliferation, surface hydration, or cellular organization between the ECSS and FCSS groups. Both groups exhibited excellent stratification with a continuous layer of basal keratinocytes present at the dermal–epidermal junction. After grafting to full thickness wounds in athymic mice, both skin substitutes had high rates of engraftment: 87.5% in the FCSS group and 100% in the ECSS group. Histological evaluation of wounds revealed that bovine collagen persisted in the wound at week 8 in the FCSS group while no bovine collagen was seen in the ECSS group. At 8 weeks post-grafting, the ECSS grafts were $61.3 \pm 7.9\%$ original graft area whereas the FCSS grafts were $39.2 \pm 8.8\%$ original area ($p < 0.01$). These results indicate that ES scaffolds can be used to fabricate skin substitutes with optimal cellular organization and can potentially reduce wound contraction compared to FD scaffolds. These advantages may lead to reduced morbidity in patients treated with skin substitutes fabricated from ES collagen.

Keywords: Wound healing; Collagen; Scaffold; Wound closure

1. Introduction

In severely burned patients, the prompt closure of full thickness wounds is critical for survival. Split thickness skin grafts are commonly grafted to the wound to promote recovery [1,2]. Limited donor sites and the potential advantages of reduced numbers of surgical procedures and donor site surface area are the major impetus for development of bioengineered skin. Tissue engineering has been utilized to generate bioengineered substitutes for skin which produce greater expansion of surface area from donor skin than conventional methods [3]. In both clinical and preclinical models of skin substitutes, collagen is the most commonly used scaffolding material [4–7] due to its many advantageous properties, including low antigenicity and promotion of cell attachment and growth.

For wound management, freeze-dried (FD) collagen sponges are frequently placed onto wounds without cells [8,9], in conjunction with fibroblasts [4,10–12], or populated with keratinocytes and fibroblasts [13–15]. Previous studies have shown collagen sponges and cell-populated collagen sponges were able to promote wound healing [9,16–18]. To fabricate the collagen sponge, a suspension of collagen in acetic acid is solidified by freezing. The collagen

*Corresponding author. 3229 Burnet Avenue, Shriners Hospitals for Children, Cincinnati, OH 45229, USA. Tel.: +1 513 872 6076; fax: +1 513 872 6229.
E-mail address: hpowell@shrinenet.org (H.M. Powell).

0142-9612/$ - see front matter © 2007 Elsevier Ltd. All rights reserved.
doi:10.1016/j.biomaterials.2007.10.036

is displaced by developing ice crystals, which form continuous networks of ice and collagen [19]. Subsequent sublimation of the ice crystals generates a highly porous sponge. The pore size and structure depend on the nucleation and growth rate of ice crystals during the freezing process. The formation of ice crystals is primarily controlled by the undercooling of the collagen suspension by an inverse relationship where higher nucleation rates and slower protein diffusion lead to smaller pores [20]. Rapid, quench freezing processes are commonly used in sponge fabrication and lead to variable heat transfer to the solution, generating sponges with a heterogeneous pore structure and large variation in pore diameter at different locations in the scaffold [20]. In addition, the collagen sponge is structurally different than natural extracellular matrix (ECM). Native ECM is fibrillar in structure with micron to submicron sized fibers, while collagen sponges are comprised of a reticulated network of partially denatured collagen with pore walls several microns thick. Thus, alternative methods of scaffold fabrication that are more homogeneous and biomimetic are needed.

To generate scaffolds with greater homogeneity and homology to natural ECM, electrospinning has been utilized to produce a fibrous matrix consisting of submicron to nanometric sized fibers. Electrospinning is an inexpensive process that has been used to fabricate nonwoven fibrous scaffolds out of a wide array of materials, including collagen [21–25]. In electrospinning, polymer solution is pumped through an aperture (i.e. syringe needle) that is electrically charged. A charge is induced on the liquid droplet at the tip of the needle by the electric potential between the needle and a grounded collection plate. When the electric field reaches a threshold, the repulsive electric force within the liquid overcomes the surface tension of the solution, causing a charged jet of solution to be ejected from the droplet of polymer solution [22]. The polymer jet is then accelerated toward the target, which is oppositely charged or grounded. This process generates nonwoven meshes composed of nanometric to micron-sized fibers. Fiber diameter and morphology of the electrospun (ES) scaffold are largely controlled by concentration and molecular weight of the polymer [26–29]. Many other factors, including flow rate, quality of the solvent, and surface tension result in variation of fiber diameter and morphology [22]. By altering these factors, a nonwoven mesh with a fibrous structure similar to native ECM can be generated with narrow tolerances.

This study evaluates the use of ES collagen scaffolds for the preparation and transplantation of human skin substitutes. Skin substitutes were fabricated utilizing either ES collagen or FD collagen scaffolds. Cell distribution, proliferation, organization, and maturation on each scaffold type were evaluated and the ability of the resultant skin substitutes to engraft and heal full thickness wounds athymic mice was assessed.

2. Materials and methods

2.1. Collagen scaffolds

FD and ES collagen scaffolds were prepared from comminuted bovine hide collagen (Kensey Nash; Exton, PA). For collagen sponges, fibrous bovine collagen powder (SEMED F; 0.60% wt./vol.) was homogenized in 0.5 M acetic acid, cast into sheets, frozen, and lyophilized as previously described [30] but without lamination. ES collagen scaffolds were fabricated using a 10% wt./vol. solution of acid-soluble collagen (SEMED S) in hexafluoropropanol (HFP; Sigma, St. Louis, MO). Matrices were spun at a potential of 30 kV onto an 8.5 cm^2 grounding plate that was positioned perpendicular to the tip of the needle. The ES and FD scaffolds were physically crosslinked by vacuum dehydration at 140 °C for 24 h [31], then chemically cross-linked in a solution of 5 mM 1-ethyl-3-3-dimethylaminopropylcarbodiimide hydrochloride (EDC; Sigma, St. Louis, MO) in 100% ethanol for 24 h. The scaffolds were then disinfected in 70% ethanol for 24 h and rinsed thoroughly following a procedure previously described [7] in preparation for cell inoculation.

2.2. Scanning electron microscopy

The morphology of the FD and ES scaffolds was examined by scanning electron microscopy (Hitachi S-3000). Punch biopsies from dry scaffolds were collected from six distinct regions within a scaffold and mounted onto aluminum stubs, sputter coated with gold-palladium and imaged in secondary electron mode with a 5 kV accelerating voltage. Images were collected; homogeneity of the scaffolds was assessed qualitatively and fiber diameter of ES scaffolds was assessed quantitatively.

2.3. Preparation of skin substitutes

Skin substitutes were prepared from FD and ES collagen scaffolds populated with human dermal fibroblasts (HF) and epidermal keratinocytes (HK) isolated from surgical discard tissue with Institutional Review Board approval. HF were inoculated onto ES or FD scaffolds, cut into 6.5 × 6.5 cm^2, at a density of 5.0×10^5 cells/cm^2 and incubated at 37 °C and 5% CO_2 in UCMC 160 medium [32] for 2 days. Scaffolds were then inoculated with HK at a density of 1.0×10^6 cells/cm^2. One day following HK inoculation (skin substitute incubation day 1), the cell-scaffold constructs were placed onto a perforated stainless steel platform covered by a cotton pad to establish an air–liquid interface and incubated up to 21 days with the skin substitute culture media replaced daily. All experiments were conducted utilizing a total of three different donor cell strains.

2.4. Fluorescein diacetate (FdA) staining

FdA has been previously used in a preclinical model to determine the viability and distribution of cells within cultured skin substitutes [33]. FdA penetrates the cell membrane and remains colorless until the acetate moieties in FdA are cleaved nonspecifically by esterases that convert the nonfluorescent FdA to fluorescein [34]. Thus, the viable cells can be visualized when the intracellular FdA is exposed to ultraviolet light (366 nm) [35,36] and intensity of fluorescence is proportional to the number of viable cells. To visualize the distribution of cells on the ES and FD scaffolds, skin substitutes fabricated using these two scaffolds were stained with FdA 1 day following HK inoculation. A freshly diluted solution of FdA (0.04 mg/ml) in phosphate buffered saline (PBS) was prepared, vacuum filtered, and warmed at the time of the assay. The skin substitutes were immersed in the FdA solution for 20 min, then samples were transferred to an empty 150 mm culture dish (Corning Inc.; Corning, NY) for photography. A UV lightbox (Fisher BioTech.; Pittsburgh, PA) illuminated the skin substitutes and the resultant fluorescence was captured on Polaroid black and white film type 667 (Sigma; St. Louis, MO). A photograph of each skin substitute was scanned and analyzed using Metamorph software program (Molecular Devices Corporation;

Downington, PA). For each sample average, maximum and minimum fluorescence intensities were calculated. Homogeneity of cell distribution was quantified by dividing the maximum fluorescence intensity value by the minimum fluorescence intensity value; a value of 1 was equal to a 100% homogeneous distribution of cells.

2.5. Surface electrical capacitance (SEC) measurement

SEC directly measures skin surface hydration, which is related to barrier function [37,38]. SEC measurements were collected from the skin substitutes *in vitro* using the NOVA dermal phase meter (DPM 9003; NOVA Technology; Portsmouth, NH), with low SEC readings corresponding to reduced levels of surface hydration: an indicator of functional epidermal barrier. On culture days 7, 14, and 21, measurements were collected from three sites on each skin substitute (6 grafts per cell strain $\times 3$ cell strains = 18 skin substitutes per group $\times 3$ measurements per graft = 54 measurements per group) and the SEC values are expressed in DPM units as mean ± standard error (SEM). SEC readings from normal human skin were collected from the volar forearm of healthy volunteers.

2.6. Histology

To determine the local variation of pore size in FD and ES scaffolds ($n = 6$ per group), hydrated scaffolds were embedded in OCT™ compound (Sakura Finetek; Torrance, CA) *en face* and cryo-sectioned ~7 μm thick at 20 μm intervals using standard histological procedures. The sections were stained with aniline blue and imaged with a Nikon FXA photomicroscope (Melville, NY). Image J was used to measure the pore areas from the brightfield images. Six distinct sections from each sample were imaged (8 images per sample) and pore areas were calculated for each sample. Data are presented as pore area mean ± SEM. For the ES scaffolds, a pore was defined by the area enclosed by fibers in a given 7 μm thick plane.

Biopsies for histology from freeze-dried collagen skin substitutes (FCSS) and electrospun collagen skin substitutes (ECSS), collected at days 7, 14, and 21, were fixed in formalin for 1 h prior to processing and paraffin embedding. Sections were stained with hematoxylin and eosin (H&E) and imaged with light microscopy. Bright field images were collected with SPOT Advanced Imaging software (Diagnostic Instruments; Sterling Heights, MI) with a total of nine samples per condition per time point. From images taken of samples at day 7, the depth of cell penetration was measured using Image J software. Average penetration depth for each sample was calculated from three distinct measurements on sections on each sample. A total of nine samples per condition were measured and results reported as average penetration depth ± SEM.

To visualize basement membrane formation and epidermal differentiation markers biopsies were collected at days 7 and 14 for cryosectioning. Cryosections were fixed in methanol for 8 min followed by acetone for 2 min. After fixation, the samples were immunostained for human involucrin (Sigma; St. Louis, MO) and human collagen type IV (Biodesign International; Saco, ME). The double labeled sections were examined via epi-fluorescence microscopy (Nikon Microphot FXA; Melville, NY) and images were collected with SPOT Advanced imaging software with a total of six specimens per condition per time point.

2.7. Bromo-deoxyuridine (BrdU) labeling

To determine the proportion of cells in the *in vitro* skin substitutes which were actively proliferating, FCSS and ECSS were exposed to medium containing 65 μg BrdU for 24 h prior to sample collection. Samples were taken at day 7 *in vitro*, embedded in OCT™ compound and processed for cryosectioning. Slides were then fixed in methanol for 8 min followed by acetone for 2 min and rehydrated in PBS. The sections were co-labeled with anti-BrdU-fluorescein isocyanate antibody (BD Biosciences; Franklin Lakes, NJ) and anti-pan-cytokeratin antibody (Invitrogen; Carlsbad, CA) by overnight incubation at 4 °C. The double-labeled sections were then examined microscopically, a total of 90 fields of view were examined per group. The number of BrdU positive cells per microscopic field was recorded and data presented as the number of BrdU positive cells per field (mean ± SEM).

2.8. Grafting of CSS to athymic mice

All procedures using animals were approved by University of Cincinnati Institutional Animal Care and Use Committee and followed NIH guidelines. At culture day 14, skin substitutes made with FD or ES scaffolds were grafted onto $2 \times 2\,cm^2$ full thickness wounds prepared surgically in female athymic mice (nude-Foxn1^{nu}; Harlan, Indianapolis, IN; $n = 8$ for ECSS, $n = 7$ FDSS). An occlusive dressing with antibiotic ointment was applied to the graft as previously described [39]. At 2 weeks after surgery, dressings and stent sutures were removed and animals were maintained without dressings for the remainder of the assessment period.

2.9. Animal data collection and analysis

Photographs and tracings of the wound areas were collected at weekly intervals of 2–8 weeks by placing sterile tracing paper over the wound and manually outlining the wound perimeter. Wound area was then quantified using computer planimetry and percent original area defined as wound area at a specific time point divided by the initial wound area $\times 100$. Data are presented as percent original area (mean ± SEM).

All animals were euthanized at week 8 and two graft biopsies were collected from each animal, with one processed for paraffin embedding and another for cryosections. The paraffin sections were H&E and Masson Trichrome stained to assess cellular organization and to determine the persistence of the bovine collagen sponge. Cryosections were used to confirm engraftment of human keratinocytes via immunohistochemical staining for HLA-ABC antigens [39,40]. The percentage of grafts on animals with HLA-ABC positive keratinocytes at week 8 is expressed as percent HLA-positive wounds. In addition, cryosections were immunostained for mouse CD31 (BD Biosciences) to visualize vascularization of the engineered skin substitutes and human collagen type IV (Biodesign International) for basement membrane formation.

2.10. Statistical analysis

For quantitative assays either repeated measures ANOVA or Student's *t*-tests were performed. The data were presented as mean ± SEM with a $p < 0.05$ considered statistically significant.

3. Results

3.1. Scaffold morphology

Scaffolds fabricated via freeze-drying methods showed local structural differences in pore area with an average pore area of $618.4 \pm 87.5\,\mu m^2$ and a range of 17–1898 μm^2 (Figs. 1(A) and (B)). In contrast, ES scaffolds did not possess considerable local variation in structure (Figs. 1(C) and (D)). Pore areas in ES scaffolds ranged 22–1413 μm^2 with an average of $396.0 \pm 59.7\,\mu m^2$. FD scaffolds contained large pores separated by 1–10 μm thick reticulations whereas ES scaffolds were nonwoven meshes with fibers 1.3 μm in diameter on average and ranged from 0.13 to 4.5 μm. Scanning electron microscopy did reveal major differences in the density of the scaffolds. FD scaffolds were much more porous than the ES scaffolds;

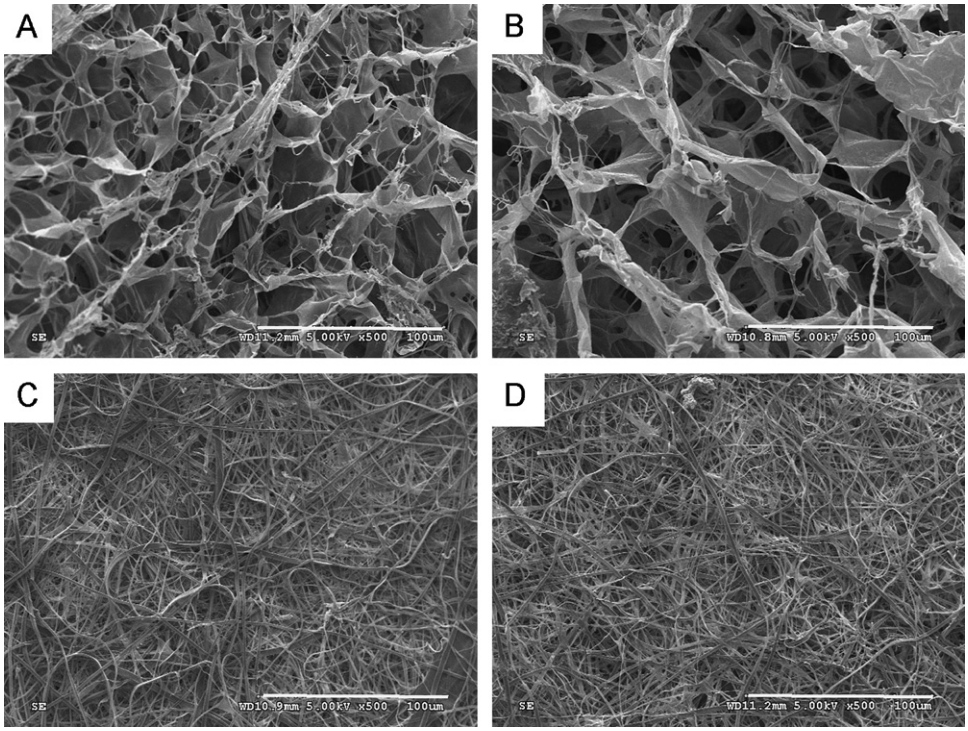

Fig. 1. SEM images of freeze-dried (A,B) and electrospun (C,D) collagen scaffolds taken from different regions within the scaffold. Note the spatial difference in pore size of the freeze-dried scaffold. Scale bars = 100 μm.

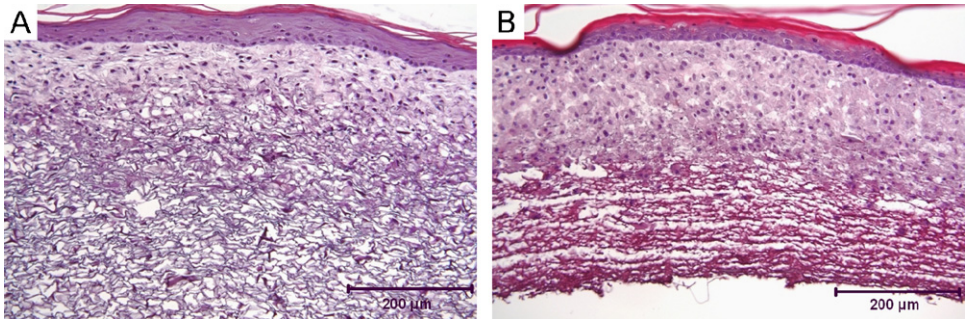

Fig. 2. Histological images of (A) freeze-dried collagen skin substitutes (FCSS) and (B) electrospun collagen skin substitutes (ECSS) at day 7. Fibroblasts and keratinocytes were well stratified on both scaffolds with a continuous basal layer of keratinocytes present in both. A layer of cornified keratinocytes was forming in both. Scale bar = 200 μm.

however, the ES scaffolds fibers were not joined to one another (Fig. 1).

3.2. Co-culture of HK and HF on FD and ES collagen

FdA staining of skin substitutes prepared with FD (FCSS) and ES (ECSS) collagen scaffolds indicated no statistical difference in cell distribution at day 1 between the two scaffolds types, with a 2.43× average variation in cell density in the FCSS and a 2.8× average variation in the ECSS. Histological images at day 7 and day 14 showed dense populations of fibroblasts present in both scaffolds (Figs. 2(A) and (B)) with the fibroblasts in both scaffolds remaining in the upper regions of the matrix. Fibroblasts penetrated an average of 163.6 ± 7.6 μm into the FD scaffolds by 7 days in culture whereas CF penetration depth was 183.3 ± 14.0 μm in the ES group ($p = 0.1185$). Well stratified dermal and epidermal layers and continuous basal cell layers were present in both (Figs. 2(A) and (B)).

As the FCSS and ECSS matured at the air–liquid interface, the epithelium keratinized (Figs. 2(A) and (B)), began to form an epidermal barrier and caused the surface of the material to dry. SEC measurements (DPM units) of both groups at day 7 revealed the surface of the skin substitutes was still moist and had not yet fully matured. By day 14, surface hydration decreased in both groups, nearing normal human skin levels (Fig. 3). After incubation for 21 days at the air–liquid interface, both the FCSS and ECSS were not statistically different from normal human skin for surface hydration (Fig. 3, dotted line).

Analysis of cell proliferation via BrdU labeling revealed no statistically significant differences in cell proliferation

between the FCSS and ECSS at day 7 ($p > 0.05$). The FDSS had 18.1 ± 2.6 BrdU-positive cells per field of view while 18.7 ± 1.9 BrdU-positive cells were present in each field of view in the ECSS (data not shown). Immunostaining for involucrin, a cytoplasmic protein precursor of the epidermal cornified envelope, showed positive staining for involucrin in all the epidermal layers except for the basal cell layer in both the FDSS and ECSS (Figs. 4(B) and (F)). Basement membrane formation was evident in both the FDSS and ECSS as indicated by the continuous layer of collagen IV at the dermal–epidermal junction in the skin substitutes *in vitro* (Figs. 4(C) and (G)).

3.3. Wound closure on athymic mice

Fig. 5 shows representative animals from each group at 2 and 8 weeks after grafting. At 2 weeks after surgery, grafts prepared with FD and ES scaffolds were well integrated into surrounding murine skin and possessed a uniformly dry epidermis (Figs. 5(A) and (B)). By 8 weeks, the FCSS and ECSS grafts were visibly smaller with a majority of the ECSS maintaining their original shape (Figs. 5(C) and (D)). Differences in surface area between the FCSS and ECSS groups were observed with the ECSS grafts on average larger than the FCSS.

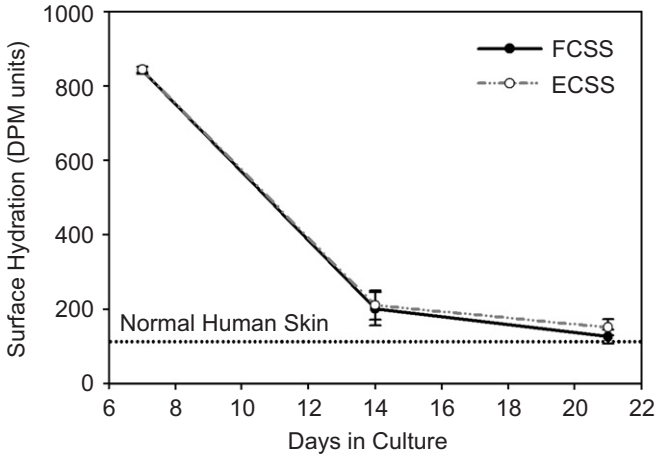

Fig. 3. Surface electrical capacitance of FCSS and ECSS as a function of time. By day 14 in culture both skin substitutes had rapid decreases in surface hydration and were approaching normal human skin levels.

3.4. Microscopic examination of healed wounds

At 8 weeks after surgery, microscopic evaluation of a skin biopsy collected from each animal showed excellent cell migration into the dermal component of both graft types (Figs. 6(A)–(D)). The healed grafts displayed a thick, keratinized epidermis in the FCSS and ECSS. However, the ECSS group displayed a non linear dermal–epidermal junction reminiscent of rete ridges found in normal human skin (Figs. 6(C) and (D)). Undigested bovine collagen sponge was visible in within the graft on animals from the FCSS group (Figs. 6(A) and (B) arrows) but no particulates of ES bovine collagen could be seen in the mouse skin (Fig. 6(B)). In contrast, no residual ES collagen was found in any of the ECSS animals at week 8 and the dermal component of the grafted ECSS and the murine skin were similar in appearance (Fig. 6(D)).

Immunostaining for HLA-ABC confirmed engraftment of human keratinocytes occurred in all the wounds treated with ESSS (7/7) and in 87.5% of wounds treated with FCSS (7/8). The human leukocyte antigen was present throughout the graft and up to the junction between the human and mouse skin (Figs. 7(B) and (E)). CD31 staining shows vascularization of both graft types by the mouse with newly formed blood vessels present in the graft up to the dermal–epidermal junction. Human collagen IV was also present at the dermal–epidermal junction in both graft types (Figs. 8(B) and (E)) forming the basement membrane. No significant difference in collagen IV or blood vessel density and distribution was detected between the FCSS and ECSS groups.

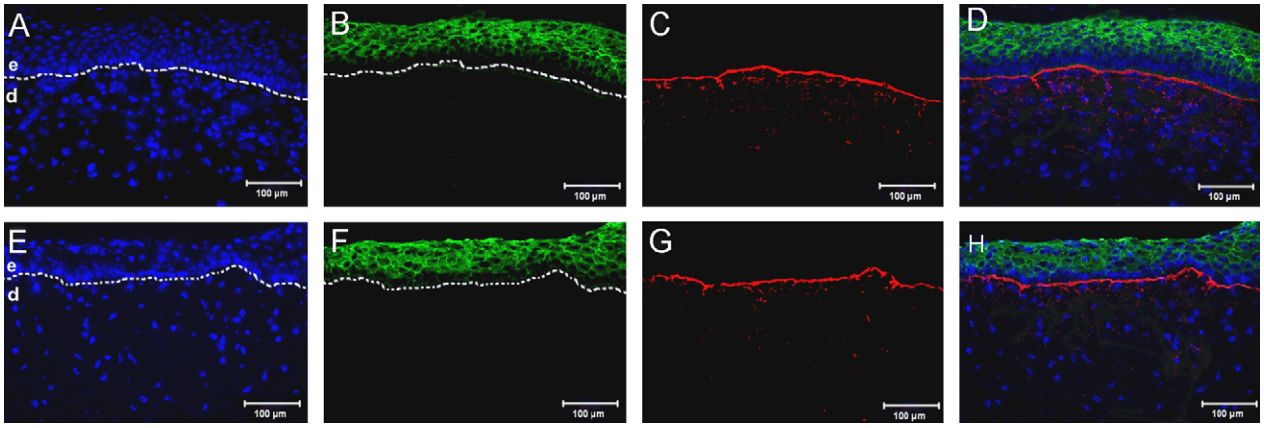

Fig. 4. Immunohistological images of FCSS (A–D) and ECSS (E–H) showing cell nuclei (A,E), human involucrin (B,F), human collagen type IV (C,G), and merged images (D,H). Epidermis and dermis are denoted by e and d, respectively. The dashed line indicates the dermal–epidermal junction. Scale bar = 100 µm.

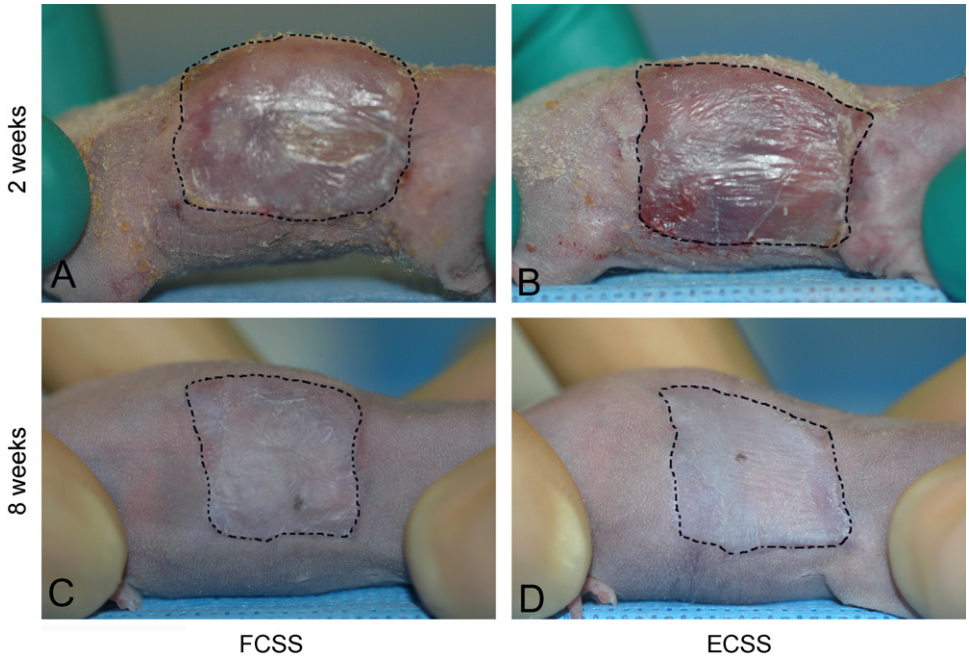

Fig. 5. Appearance of grafts on athymic mice 2 and 8 weeks after grafting. Skin substitutes fabricated using freeze-dried (FCSS; A,C) or electrospun collagen (ECSS; B,D) at 2 weeks (A,B) or 8 weeks (C,D), respectively. Wound areas are traced with a dashed black line.

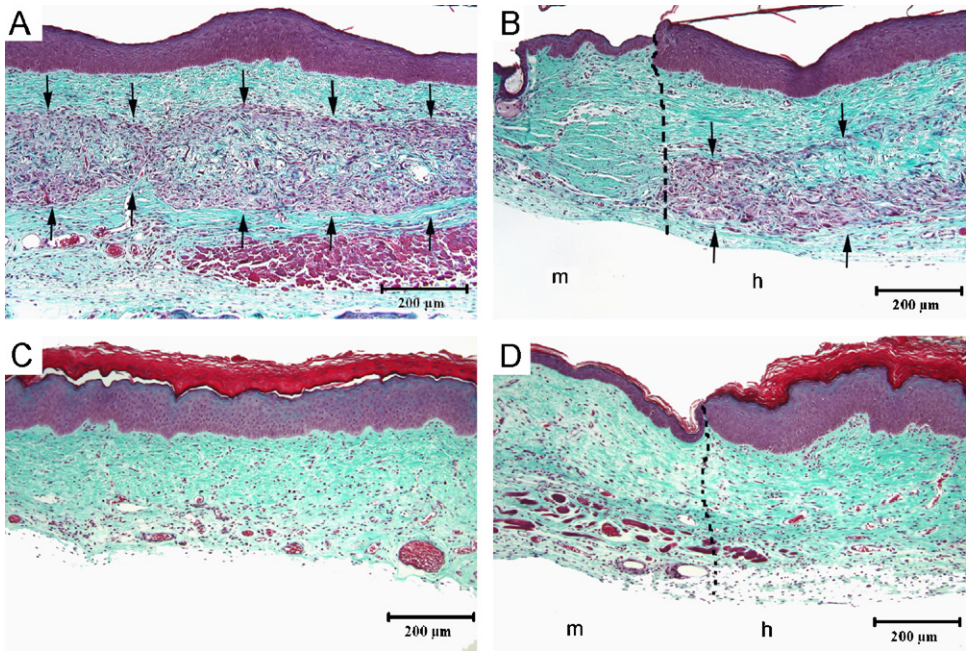

Fig. 6. Histological examination of healed skin 8 weeks after grafting. Masson trichrome staining of (A,B) FCSS and (C,D) ECSS after grafting to athymic mice for 8 weeks. Dashed line (B,D) follows the border between murine and human skin. Residual freeze-dried collagen scaffolds can be seen in the wound grafted with FCSS (dark purple staining; arrows). Scale bar = 200 μm.

3.5. Wound area after grafting

A plot of percent original area versus time showed a time dependent reduction in wound area (Fig. 9). Both FCSS and ECSS wounds contracted rapidly until week 4 when the ECSS group began to stabilize. The FCSS group continued to slowly contract until week 8. At week 8 the FCSS grafts had contracted to $39.2 \pm 8.8\%$ of their original areas whereas the ECSS group contracted to $68.8 \pm 2.8\%$ of its original area ($p < 0.01$).

4. Discussion

Scaffold pore size, pore orientation, fiber structure, and fiber diameter have been shown to regulate proliferation, cellular organization, and subsequent tissue

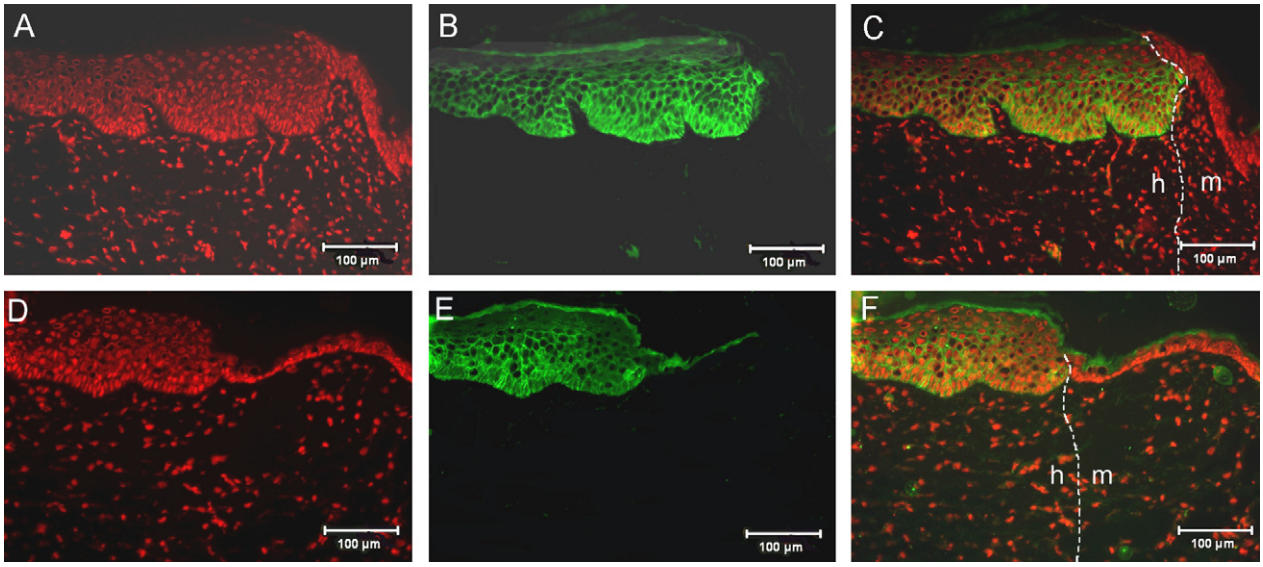

Fig. 7. Immunohistological images of FCSS (A–C) and ECSS (D–F) showing the cell nuclei (A,D), HLA-ABC present only in human skin (B,E), and merged images (C,F). The dashed line indicates the junction between the human (h) and mouse (m) tissue. Scale bar = 100 μm.

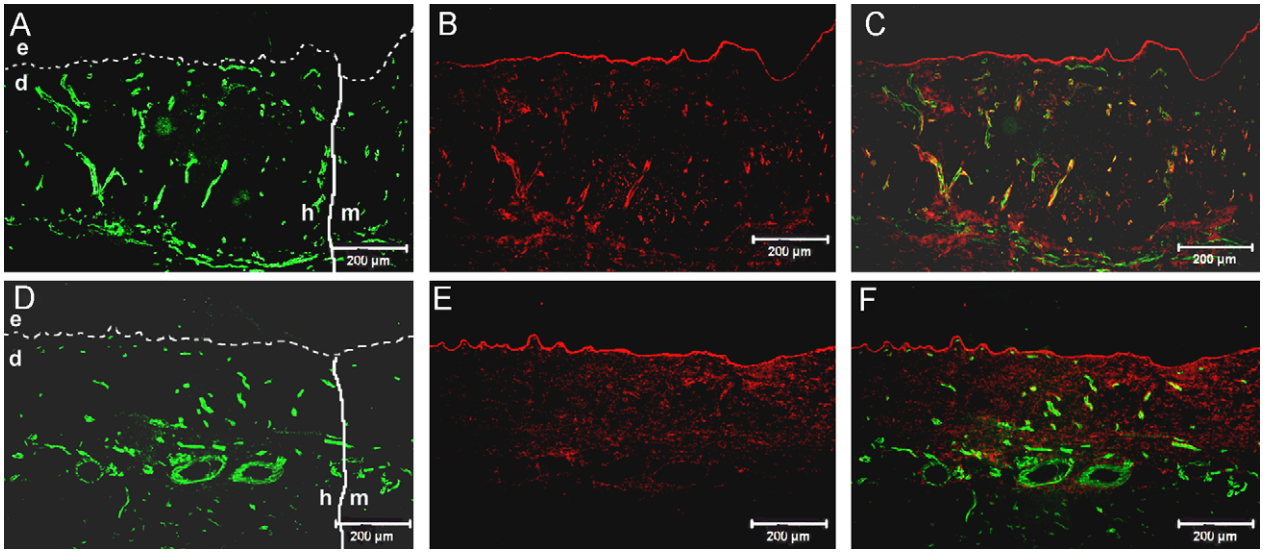

Fig. 8. Distribution and density of newly formed blood vessels in the FCSS (A–C) and ECSS (D–F) were assessed using a monoclonal antibody for mouse CD31 (A,D). Human collagen type IV is shown in (B,E) with merged images in (C,F). The vertical line indicates the junction between the human (h) and mouse (m) tissue. Scale bar = 200 μm.

morphogenesis [41–44]. Although the structure of the FD and ES scaffolds were markedly different (Fig. 1), cell proliferation and organization were similar on both scaffolds. The ES scaffolds contained pores that were on average half the area of the FD scaffolds, yet cell penetration was comparable between the two scaffold types (Fig. 2). A possible explanation for this phenomenon is that the cells can more easily move or maneuver around the nonwoven fibers, which comprised the ES scaffolds, as they are not joined. In contrast, the pores of the FD scaffolds, which consisted of continuous reticulations of collagen, cannot be as easily penetrated by the cells. It is apparent that proper selection of pore size and porosity depends not only on target tissue but also scaffold structure, i.e. sponge, woven mesh or nonwoven mesh.

In addition to similar rates of proliferation, both scaffolds types generated skin substitutes which formed basement membrane *in vitro* as evidenced by a continuous layer of collagen IV at the dermal–epidermal junction. The distribution and intensity of the stain was similar in both groups (Figs. 4(C) and (G)) which would be expected as both groups produced skin substitutes with similar cellular organization and stratification of the cell types. As the skin substitutes mature at the air liquid interface, the keratinocytes in the epidermis stratify and differentiate to form basal, spinous, and granular layers with an overlying

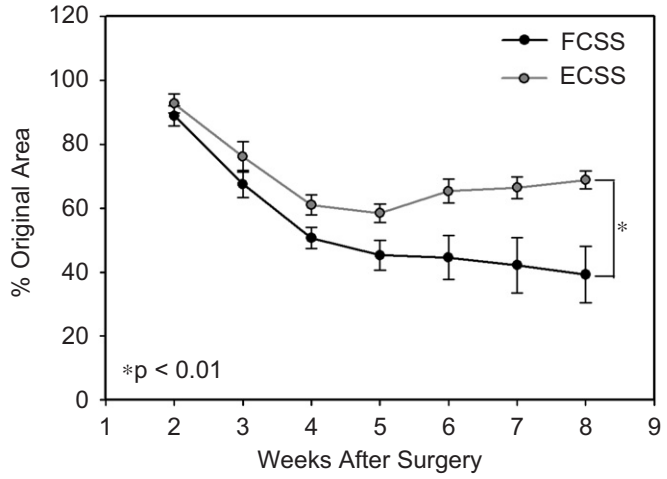

Fig. 9. Percent original wound area versus time for wounds grafted with FCSS or ECSS. Both had similar rates of wound contraction up to 4 weeks post-surgery, after which the ECSS wound area stabilized but the FCSS continued to contract. At 8 weeks post-surgery, the wounds grafted with ECSS were larger in area than the FCSS group.

stratum corneum. As the keratinocytes migrate out of the basal cell layer towards the surface of the skin, they lose the ability to divide, and terminally differentiate [45]. During this process, differentiation-dependent proteins are synthesized, including involucrin, a cytoplasmic protein precursor of the cornified envelope. Involucrin is found in the upper spinous layers *in vivo* [46,47]. In the engineered skin substitutes involucrin is found directly above the basal cell layer through the stratum corneum in both groups, indicating that the keratinocytes within the epidermis are differentiating. Although the engineered skin substitutes attempt to restore native skin anatomy, it is apparent that the involucrin distribution within the skin substitute is vastly different than *in vivo*. It has been previously shown that engineered skin substitutes have a gene expression profile that is more analogous to wounded native skin than normal human skin [48]. As the keratinocytes are hyperproliferative within the skin substitutes, it is not surprising that involucrin would be present in all the epithelial layers except for the basal layer as the epidermis would be rapidly differentiating. A similar pattern of involucrin staining has been also reported in other skin substitutes grafted to athymic mice [49].

When grafted to full thickness wounds in athymic mice, both skin substitutes had high rates of engraftment; 87.5% in the FCSS group and 100% in the ECSS group. Each group was well integrated into the hosts tissue. A thick human epidermis was present and no disjunction was found at the border between the human and mouse tissue in both groups (Figs. 6(B) and (D)). Histologically, the bovine collagen scaffold in the FCSS group persisted at week 8 (Figs. 6(A) and (B)) while no bovine collagen was observed in the ECSS group (Figs. 6(C) and (D)). This could be due to the greater solubility of the starting material or the higher surface area to bulk ratio in the fibrous ES scaffold. Both scaffolds are fabricated using collagen from comminuted bovine hide; however the collagen for electrospinning is a more acid-soluble form (SEMED S) to enhance the solubility of the collagen in the HFP. The fibrous collagen used for sponge fabrication is less soluble and both scaffold types are chemically cross-linked with EDC which further increases the scaffolds resistance to degradation. In addition, the large surface area to volume ratio of the fibers in the ES scaffolds could also allow them to be degraded at a more rapid rate than the bulky FD scaffold which had a lower surface area to volume ratio. However, the presence of FD collagen within the wound did not appear to hinder the vascularization of the skin substitute as mouse blood vessels were present in the entire dermis as was also the case in the ECSS group.

The most interesting observation was reduction in wound contraction in the ECSS group compared to that of the FCSS group, indicating greater ECSS graft stability. At 8 weeks post-grafting, the ECSS grafts were $68.8 \pm 2.8\%$ original graft area, whereas the FCSS grafts were $39.2 \pm 8.8\%$ original area. While these levels of contraction are high, it is important to note that, in a murine wound model, the skin contracts much more quickly and for a longer duration than in human skin wounds. The lower wound contraction in the ECSS group, which appears to have the highest scaffold degradation rate, is in contrast to previous reports that state wound contraction was slowest in wounds grafted with more stable material [44]. However, these reports investigated acellular materials. It is possible that the higher turnover rate of collagen in the ECSS healed wounds promoted more rapid infiltration of host cells to the wound and more prompt wound stabilization. However it is difficult to determine this currently as wound biopsies from earlier time points were not collected. In future investigations, biopsies would be collected at multiple time points to better assess the *in vivo* degradation rate of the scaffolds.

5. Conclusions

Electrospinning is a process that can be used to fabricate collagen scaffolds economically at large scales. These results indicate that ES collagen scaffolds can be used to fabricate skin substitutes with optimal cellular organization. ES scaffolds have been shown to produce skin substitutes with similar cellular organization, proliferation, and maturation to the current, clinically utilized model and were shown to reduce wound contraction, which may lead to reduced morbidity in patient outcomes.

Acknowledgments

HMP thanks the Shriners Hospitals for Children for a Post-Doctoral Research Fellowship and Grant #8450 that supported these studies. The authors would also like to thank Dr. David Witte within the Department of Pathology at the Cincinnati Children's Hospital Medical

Center for the use of their scanning electron microscopy facilities.

References

[1] Tanner JC, Vandeput J, Olley JF. The mesh skin graft. Plast Reconstr Surg 1964;34:287–92.

[2] Warden GD, Saffle JR, Kravitz M. A 2-stage technique for excision and grafting of burn wounds. J Trauma 1982;22(2):98–103.

[3] Boyce ST, Kagan RJ, Greenhalgh DG, Warner P, Yakuboff KP, Palmieri T, et al. Cultured skin substitutes reduce requirements for harvesting of skin autograft for closure of excised, full-thickness burn. J Trauma 2006;60253(4):821–9.

[4] Park S-N, Lee HJ, Lee KH, Suh H. Biological characterization of EDC-crosslinked collagen–hyaluronic acid matrix in dermal tissue restoration. Biomaterials 2003;24:1631–41.

[5] Yannas IV, Burke JF, Orgill DP, Skrabut EM. Wound tissue can utilize a polymeric template to synthesize a functional extension of skin. Science 1982;215:174–6.

[6] Hansbrough J, Boyce S, Cooper M, Foreman T. Burn wound closure with cultured human keratinocytes and fibroblasts attached to a collagen-glycosaminoglycan substrate. J Am Med Assoc 1989;262: 2125–30.

[7] Powell HM, Boyce ST. EDC crosslinking improves cultured skin substitute strength and stability. Biomaterials 2006;27(34): 5821–7.

[8] Jansson K, Haegerstrand A, Kratz G. A biodegradable bovine collagen membrane as a dermal template for human in vivo wound healing. Scand J Plast Reconstr Hand Surg 2001;35:369–75.

[9] Yannas IV, Lee E, Orgill DP, Skrabut EM, Murphy GF. Synthesis and characterization of a model extracellular matrix that induces partial regeneration of mammalian skin. Proc Natl Acad Sci USA 1989;86:933–7.

[10] Jarman-Smith ML, Bodamyali T, Stevens C, Howell JA, Horrocks M, Chaudhuri JB. Porcine collagen crosslinking, degradation and its capability for fibroblast adhesion and proliferation. J Mater Sci Mater Med 2004;15:925–32.

[11] Park S-N, Park JC, Kim HO, Song MJ, Suh H. Characterization of porous collagen/hyaluronic acid scaffold modified by 1-ethyl-3-(3-dimethylaminopropyl)carbodiimide cross-linking. Biomaterials 2002;23:1205–12.

[12] Hafemann B, Ghofrani K, Gattner H-G, Stieve H, Pallua N. Cross-linking by 1-ethyl-3-collagen/elastin membrane meant to be used as a dermal substitute: effects on physical, biochemical and biological features *in vitro*. J Mater Sci Mater Med 2001;12: 437–46.

[13] Boyce ST, Greenhalgh DG, Housinger T, Kagan RJ, Rieman MT, Childress C, et al. Skin anatomy and antigen expression after burn wound closure with composite grafts of cultured skin cells and biopolymers. Plast Reconstr Surg 1993;91:632–41.

[14] Boyce ST, Goretsky M, Greenhalgh DG, Kagan RJ, Rieman MT, Warden GD. Comparative assessment of cultured skin substitutes and native skin autograft for treatment of full-thickness burns. Ann Surg 1995;222(6):743–52.

[15] Kisner A, Lesiak-Cyganowska E, Sladowski D. In vitro reconstruction of full thickness human skin on a composite collagen material. Cell Tissue Bank 2001;2:165–71.

[16] Compton CC, Butler CE, Yannas IV, Warland G, Orgill DP. Organized skin structure is regenerated in vivo from collagen–GAG matrices seeded with autologous keratinocytes. J Invest Dermatol 1998;110:908–16.

[17] Powell HM, Boyce ST. Wound closure with EDC cross-linked skin substitutes grafted to athymic mice. Biomaterials 2007;28(6): 1084–92.

[18] Erdag G, Sheridan R. Fibroblasts improve performance of cultured composite skin substitutes on athymic mice. Burns 2004;30(4): 322–8.

[19] Freyman TM, Yannas IV, Gibson LJ. Cellular materials as porous scaffolds for tissue engineering. Prog Mater Sci 2001;46:273–86.

[20] O'Brien FJ, Harley BA, Yannas IV, Gibson L. Influence of freezing rate on pore structure in freeze-dried collagen-GAG scaffolds. Biomaterials 2004;25:1077–86.

[21] Reneker DH, Yarin AL, Zussman E, Xu H. Electrospinning of nanofibers from polymer solutions and melts. Adv Appl Mech 2007; 41:43–195.

[22] Chew SY, Wen Y, Dzenis Y, Leong KW. The role of electrospinning in the emerging field of nanomedicine. Curr Pharm Des 2006; 12:4751–70.

[23] Matthews JA, Wnek GE, Simpson DG, Bowlin GL. Electrospinning of collagen nanofibers. Biomacromolecules 2002;3:232–8.

[24] Matthews JA, Boland ED, Wnek GE, Simpson DG, Bowlin GL. Electrospinning of collagen type II: a feasibility study. J Bioact Compat Polym 2003;18(2):125–34.

[25] Telemeco TA, Ayres C, Bowlin GL, Wnek GE, Boland ED, Cohen N, et al. Regulation of cellular infiltration into tissue engineering scaffolds comprised of submicron diameter fibrils produced by electrospinning. Acta Biomater 2005;1:377–85.

[26] Deitzel JM, Kleinmeyer J, Harris D, Tan NCB. The effect of processing variables on the morphology of electrospun nanofibers and textiles. Polymer 2001;42(1):261–72.

[27] Gupta P, Elkins C, Long TE, Wilkes GL. Electrospinning of linear homopolymers of poly(methyl methacrylate): exploring relationships between fiber formation, viscosity, molecular weight and concentration in a good solvent. Polymer 2005;46(13):4799–810.

[28] Zong X, Kim K, Fang D, Ran S, Hsiao BS, Chu B. Structure and process relationship of electrospin bioabsorbable nanofibers membranes. Polymer 2002;43:4403–12.

[29] Powell HM, Boyce ST. Fiber density of electrospun gelatin scaffolds regulates morphogenesis of dermal–epidermal skin substitutes. J Biomed Mater Res A 2007 in press.

[30] Boyce ST, Christianson DJ, Hansbrough JF. Structure of a collagen-GAG dermal skin substitute optimized for cultures human epidermal keratinocytes. J Biomed Mater Res 1988;22(10):939–57.

[31] Yannas IV. Collagen and gelatin in the solid state. J Macromol Sci Rev Macromol Chem Phys 1972;7:49–104.

[32] Swope VB, Supp AP, Schwemberger S, Babcock G, Boyce S. Increased expression of integrins and decreased apoptosis correlate with increased melanocyte retention in cultured skin substitutes. Pigment Cell Res 2006;19:424–33.

[33] Armour AD, Powell HM, Boyce ST. Fluorescein diacetate for determination of cell viability in tissue-engineered skin. Tissue Eng 2007 submitted for publication.

[34] Altman SA, Randers L, Rao G. Comparison of trypan blue dye exclusion and fluorometric assays for mammalian cell viability determinations. Biotechnol Prog 1993;9:671–4.

[35] Clarke JM, Gillings MR, Altavilla N, Beattie AJ. Potential problems with fluorescein diacetate assays of cell viability when testing natural products for antimicrobial activity. J Microbiol Methods 2001;46: 261–7.

[36] Poole CA, Brookes NH, Clover GM. Keratocyte networks visualized in the living cornea using vital dyes. J Cell Sci 1993;106: 685–92.

[37] Goretsky M, Supp AP, Greenhalgh DG, Warden GD, Boyce S. Surface electrical capacitance as an index of epidermal barrier properties of composite skin substitutes and skin autografts. Wound Repair Regen 1995;3:419–25.

[38] Boyce ST, Supp AP, Harriger MD, Pickens WL, Hoath SB. Surface electrical capacitance as a noninvasive index of epidermal barrier in cultured skin substitutes in athymic mice. J Invest Dermatol 1996; 107(1):82–7.

[39] Swope VB, Supp AP, Boyce ST. Regulation of cutaneous pigmentation by titration of human melanocytes in cultured skin substitutes grafted to athymic mice. Wound Repair Regen 2006;10:378–86.

[40] Harriger MD, Supp AP, Warden GD, Boyce ST. Glutaraldehyde crosslinking of collagen substrates inhibits degradation in skin

substitutes grafted to athymic mice. J Biomed Mater Res 1997;35: 137–45.
[41] Glicklis R, Shapiro L, Agabaria R, Merchuk J, Cohen S. Hepatocyte behavior within three-dimensional porous alginate scaffolds. Biotechnol Bioeng 2000;67:344.
[42] Ma T, Li Y, Yang S-T, Kniss D. Effects of pore size in 3-D fibrous matrix on human trophoblast tissue development. Biotechnol Bioeng 2000;70:606–18.
[43] Wang H, Pieper J, Peters F, vanBlitterswijk C, Lamme E. Synthetic scaffold morphology controls human dermal connective tissue formation. J Biomed Mater Res A 2005;74A:523–32.
[44] Salem A, Stevens R, Pearson R, Davies M, Tendler S, Roberts C, et al. Interaction of 3T3 fibroblasts and endothelial cells with defined pore features. J Biomed Mater Res 2002;61: 212–7.
[45] Van Duijnhoven JL, Schalkwijk J, Kranenborg MH, van Vlijmen-Willems IM, Groeneveld A, van Erp PE, et al. MON-150, a versatile monoclonal antibody against involucrin: characterization and applications. Arch Dermatol Res 1992;284(3):167–72.
[46] Griffin EF, Harris H. Total inhibition of involucrin synthesis by a novel two-step antisense procedure. Further examination of the relationship between differentiation and malignancy in hybrid cells. J Cell Sci 1992;102:799–805.
[47] Carroll JM, Albers KM, Garlick JA, Harrington R, Taichman LB. Tissue- and stratum-specific expression of the human involucrin promoter in transgenic mice. Proc Natl Acad Sci USA 1993;90(21): 10270–4.
[48] Smiley AK, Klingenberg JM, Aronow BJ, Boyce ST, Kitzmiller WJ, Supp DM. Microarray analysis of gene expression in cultured skin substitutes compared with native human skin. J Invest Dermatol 2005;125:1286–301.
[49] Greer DJ, Swartz DD, Andreadis ST. In vivo model of wound healing based on transplanted tissue-engineered skin. Tissue Eng 2004;10(7/8):1006–17.